

PCCP

Accepted Manuscript



This is an *Accepted Manuscript*, which has been through the Royal Society of Chemistry peer review process and has been accepted for publication.

Accepted Manuscripts are published online shortly after acceptance, before technical editing, formatting and proof reading. Using this free service, authors can make their results available to the community, in citable form, before we publish the edited article. We will replace this *Accepted Manuscript* with the edited and formatted *Advance Article* as soon as it is available.

You can find more information about *Accepted Manuscripts* in the [Information for Authors](#).

Please note that technical editing may introduce minor changes to the text and/or graphics, which may alter content. The journal's standard [Terms & Conditions](#) and the [Ethical guidelines](#) still apply. In no event shall the Royal Society of Chemistry be held responsible for any errors or omissions in this *Accepted Manuscript* or any consequences arising from the use of any information it contains.



Journal Name

COMMUNICATION

The Effect of Recombination under Short-circuit Conditions on the Determination of Charge Transport Properties in Nanostructured Photoelectrodes

Received 00th January 20xx,
Accepted 00th January 20xx

DOI: 10.1039/x0xx00000x

www.rsc.org/

J. Villanueva-Cab,^a J. A. Anta^b and G. Oskam^c

We report on the commonly unaccounted for process of recombination under short-circuit conditions in nanostructured photoelectrodes with special attention to the charge collection efficiency. It is observed that when recombination under short circuit conditions is significant, small perturbation methods overestimate the charge-collection efficiency, related to inaccurate determination of the electron diffusion coefficient and diffusion length.

Charge transport and recombination in nanostructured materials (TiO₂, ZnO, etc), commonly used as photoanodes and supporting material in solar cells such as dye or quantum dot sensitized solar cells (DSSC, QD-SSC), extremely thin absorber solar cells (ETA), perovskite-based cells, etc., determine to a large extent the performance of the devices. Special efforts have been dedicated to the relationship between the results from time-dependent and steady-state characterization techniques and phenomenological parameters, such as the electron diffusion length and electron charge collection efficiency.¹⁻⁴ The main issue is that, although devices for which a longer diffusion length is correlated with a large collection efficiency generally have a better energy conversion efficiency, the interdependence of diffusion length and collection efficiency is not straightforward.³ In addition, different research groups do not always report similar values for these parameters for similar device configurations (i.e semiconductor, dye, electrolyte) further complicating the issue. This is an important topic because in the recent surge of

the perovskite-based solar cell, the scientific community have adopted characterization techniques originally used in the DSSC field for the determination of transport and recombination kinetics,⁵⁻¹⁴ including transient photocurrent and photovoltage decay analysis, intensity-modulated photocurrent spectroscopy (IMPS), intensity-modulated photovoltage spectroscopy (IMVS) and electrochemical impedance spectroscopy (EIS). Therefore, due to the wide applicability of this type of characterization techniques, a better understanding of the parameters obtained from these methods is required, combined with an analysis of the assumptions commonly implemented in the interpretation of the results.

An important assumption that is generally made in the analysis of experimental results is that recombination does not occur under short circuit conditions, related to the observation that at 0 V the Fermi levels of the transparent conducting oxide (TCO) layers of the photoanode and counter electrode are equal. However, in general an electron density profile exists in the photoanode, even at short circuit and under illumination conditions. For example, in the dye-sensitized solar cell under illumination (1 sun), the quasi-Fermi level in the nanostructured TiO₂ film under short circuit conditions is about 0.5 eV higher than that of the TCO substrate related to the large density of trapped electrons.^{15,16} As a consequence, at short circuit and under illumination, although the potential difference between the electrodes is 0 V, the quasi-Fermi level in the TiO₂ film that is at higher energy than the redox energy, resulting in a driving force for electron transfer to the solution corresponding to a recombination process. In the dark under short circuit conditions, the quasi-Fermi level in the TiO₂ film is equal to the Fermi level of the electrodes and that of the redox mediator. To a greater or lesser extent, this should be considered as a general feature for any kind of cell with diffusion transport in the active layer. Hence, the effect of recombination under short circuit conditions, which is generally neglected, needs to be taken into account in the

^a Instituto de Física, Benemérita Universidad Autónoma de Puebla, Apdo. Postal J-48, Puebla, Pue. 72570, México. E-mail: juliovc@ifuap.buap.mx

^b Nanostructured Solar Cells Group, Department of Physical, Chemical and Natural Systems, Universidad Pablo de Olavide, Ctra. Utrera, km 1, ES-41013 Seville, Spain.

^c Departamento de Física Aplicada, CINVESTAV-IPN, Mérida, Yuc. 97310, México. Electronic Supplementary Information (ESI) available: Sample preparation, sample measurements, continuity equation solution for 660nm illumination, comparison between 660nm and Uniform illumination to obtain the real diffusion length, analytical solution for the continuity equation at steady state, geometrical constant used to calculate *D* from SLIT simulations. See DOI: 10.1039/x0xx00000x

analysis of the experimental results of charge transport and collection efficiency characterization techniques.

In order to evaluate the influence of recombination at short circuit on charge transport and collection properties, we use a numerical model that simulates the steady-state current-voltage curve and time-dependent response of a nanostructured solar cell in the absence of an electrical field with a continuity equation for the total carrier density accumulated in a photoelectrode, n .¹⁵

$$\frac{\partial n}{\partial t} = \frac{\partial}{\partial x} \left[D_0 (n/n_0)^{(1-\alpha)/\alpha} \frac{\partial n}{\partial x} \right] + G(x) - k_0 (n/n_0)^{(\beta-\alpha)/\alpha} \quad (1)$$

where n is time, t , and position, x , dependent; D_0 is the diffusion coefficient at a reference point, (normally in the dark, which is denoted by the subscript zero); k_0 is the recombination rate in dark; α is the trap energy distribution coefficient; β is the non-linear recombination factor and $G(x)$ is the position-dependent generation term. Note that in Equation (1) a position-dependent diffusion coefficient is effectively considered, defined by its density-dependence in the quasi-static approximation. Alternatively, a position-dependent diffusion coefficient can also be introduced in the context of Fokker-Planck theory as illustrated by Nissfolk et al.¹⁷ As described in this reference, the result is equivalent to ours as these authors also use the quasi-static approximation to relate D and n . All parameters in the model can be related to quantities experimentally accessible: see refs.^{5,15,18-20} for a detailed description and solution method of the total carrier density model represented by Eq.1. It is important to mention that n in Eq.1 is a generalized carrier density, and may therefore refer to a variety of situations as long as there is no drift contribution to carrier transport, for example, n is the excess electron density in a TiO₂ photoanode of a DSSC,^{15,19-21} or the total number of "excitations"²² in a nanostructured perovskite solar cell.⁵ The specific form of the diffusion and recombination terms, and their corresponding parameters, depend on the type of cell and on the nature of the transport and the recombination mechanisms. Most of the parameters can be obtained from small perturbation techniques such as IMPS/IMVS, EIS, transient/decay, and stepped light induced transient photocurrent, SLIT, measurements. See the supporting information for details on the method of extraction of parameters used in this study from a combination of UV-Vis spectroscopy, IMPS/IMVS and current voltage measurements. With adequate values for the input parameters, Eq.1 can be solved numerically with the appropriate boundary conditions^{15,19-22} in order to obtain the total density profile $n(x,t)$ as a function of time t and distance to contact x at a fixed voltage. Consequently, we can calculate the following parameters: 1) Photocurrent density vs. time; 2) density profile (or quasi-Fermi level) vs. light intensity; 3) charge collection efficiency vs. charge density (or illumination intensity); and 4) Photocurrent vs. voltage while performing a scan as a function of photovoltage.

Amaldi and Fermi defined the diffusion length as the average distance traveled by particles between recombination

events.²³ Here, we use three methods to determine this fundamental property:

1) Determination of the "small perturbation diffusion length", L_{sp} . This can be obtained from an equation derived by Bisquert and Mora-Seró that uses a small signal approximation, where the electron density changes by a small percentage with respect to a uniform background. This approximation leads to,^{15,21,24}

$$L_{sp} = \sqrt{D_0/k_0} (n/n_0)^{(1-\beta)/2\alpha} \quad (2)$$

In this case L_{sp} can be calculated when an average value of the charge density and the other parameters are known (see Table on Fig.1).

2) Determination of the diffusion length by simulation of small perturbation techniques. One of those methods is the stepped light induced transient photocurrent (SLIT) method, used to measure a diffusion time, τ_m , from the photocurrent rise observed upon a small perturbation superimposed onto a background illumination. This time can be then used to obtain the measured diffusion coefficient via $D_m = d^2/3.54 \tau_m$ (see below for an explanation of the 3.54 factor).²⁵ We have used Eq.1 in a previous publication to simulate a SLIT experiment and calculate the electron diffusion coefficient in DSSCs.¹⁵ These simulations also allow us to test the effect of recombination under short circuit conditions by changing the value of k_0 :

$$k_n = k_0 (n/n_0)^{(\beta-\alpha)/\alpha} \quad (3)$$

Since, k_n is related to a small-perturbation recombination rate constant,¹⁵ the diffusion length can be calculated:

$$L_m = \sqrt{D_m/k_n} \quad (4)$$

In the following, we consider the diffusion coefficient D_m and diffusion length L_m obtained from method 2 as measured parameters.

3) Using the average (mean) diffusion length L_{Av} proposed by Amaldi and Fermi²³, and recently used by Bisquert and Mora-Seró:²⁴

$$L_{Av} = \int_0^\infty x F(x) dx \quad (5)$$

where $F(x)$ is the probability distribution that a carrier is at position x ,

$$F(x) = (n - n_b) / \int_0^\infty (n - n_b) dx \quad (6)$$

and n_b is a background density (see below).²⁴

The charge collection efficiency, η_{coll} , is an important parameter defined as the number of charges collected in the external circuit divided by the number of photogenerated charges, which depends on the charge transport and recombination kinetics. The collection efficiency is often reported from the results of the small perturbation techniques using a simple (empirical) relationship $1 - \tau_{tr}/\tau_{rec}$, where τ_{tr} and

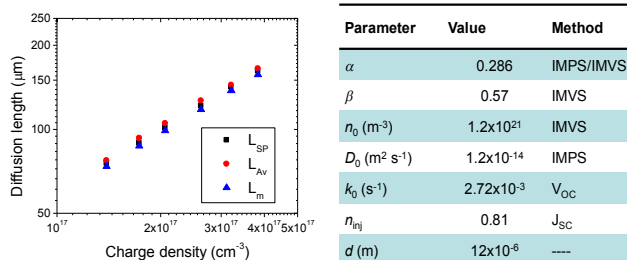


Fig. 1 Comparisons of the three methods used to calculate the electron diffusion length versus electron density for the case where recombination has a limited effect on the short circuit photocurrent (0.5%) at 1 sun illumination intensity. Table with input parameters as obtained from measurements.

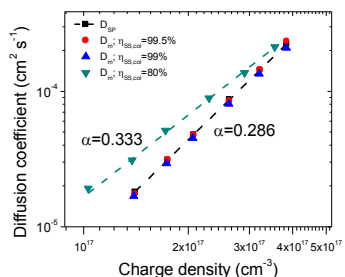


Fig. 2 Diffusion coefficient as function of charge density. Comparison between measured (IMPS) values and the model predictions for three different recombination rate constants, $k_0=0$ ($\eta_{SS, coll} = 99.5\%$ at 1 sun), $k_0=2.718 \times 10^{-3} \text{ s}^{-1}$ ($\eta_{SS, coll} = 99\%$ at 1 sun) and $k_0=0.12 \text{ s}^{-1}$ ($\eta_{SS, coll} = 80\%$ at 1 sun). When recombination takes place under short circuit conditions, the diffusion coefficient is overestimated, which can be erroneously interpreted as a trap distribution of $\alpha' = 0.333$. See text for details.

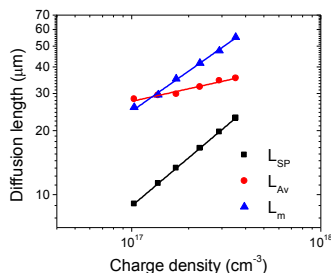


Fig. 3 Diffusion length as function of charge density when recombination results in a short-circuit photocurrent decrease by 20% ($k_0=0.21 \text{ s}^{-1}$, $\eta_{SS, coll} = 80\%$ under 1 sun illumination intensity) from the three different methods: 1) L_{sp} , small perturbation equation (Method 1), $slope = 0.752$; 2) L_m simulation (Method 2), $slope = 0.626$; and 3) L_{Av} , from the Amaldi-Fermi definition (Method 3), $slope = 0.1970$.

τ_{rec} are the electron transport and recombination times, respectively.²⁶ The validity of this relationship has been questioned recently³⁻⁴, related to the observation that the equation always seems to result in high collection efficiencies even for devices that do not have a high conversion efficiency. Hence, a detailed study is needed to determine if the small perturbation measurements are suitable for the determination of the diffusion length and collection efficiency, in particular, when recombination under short-circuit conditions is important. In the present study we also compare two different ways to obtain η_{coll} : 1) calculated from the ratio of the short circuit photocurrent density to the total charge generation

current density as obtained from the solution of **Eq.1**, called the steady state collection efficiency, $\eta_{SS, coll}$, and 2) calculated using the relation $1-\tau_{tr}/\tau_{rec}$, called the measured small perturbation collection efficiency, $\eta_{m, coll}$, where τ_{tr}/τ_{rec} is the ratio between transport and recombination times as obtained from small perturbation measurements. This collection efficiency is directly related to the measured diffusion length from small perturbation method, through the following equation:

$$\eta_{m, coll} = 1 - (1/3.54)(d/L_m)^2 \quad (7)$$

Eq.1 was solved under working conditions, i.e. under illumination with a wavelength of 660 nm, (a common wavelength used to simulate uniform illumination). We also verified that this assumption leads to similar results when a uniform generation (G is independent of x) is used (ESI). In both cases the following boundary conditions were applied:

- At $x = 0$ and $t = 0$, $n(0, 0) = n_0$
- At $x = d$, $dn/dx = 0$
- At $x = \infty$ ($x \gg d$ in the model) $n = n_b$. For a uniform generation profile, n_b is constant and determined by G . For a 660 nm LED illumination n_b should be determined by the optical length, $\lambda = \alpha_{obs}$ in the dyed film ($\alpha_{obs} = 7 \times 10^4 \text{ m}^{-1}$).

In the following discussion, Method 3 is considered to give the "real" diffusion length and will be simulated using red LED illumination. For all three methods we plot the diffusion coefficient, the diffusion length and the charge collection efficiency versus the average electron charge density. The average charge density was obtained by integration of the charge density profile at a given J_{SC} or light intensity.

For further reference, Method 3 was first tested for the simple case when the diffusion coefficient, the recombination rate, and the diffusion length are all constants (i.e., independent of the charge density), hence, with no effects of trapping ($\alpha = 1$), and using a linear dependence of recombination with charge density ($\beta = 1$). For this specific case, there is an analytical solution for **Eq.1** (ESI). It was confirmed that the parameters mentioned above were indeed the same for the three methods using our method for the case $\alpha = \beta = 1$.

In principle all three methods should converge to the same value of the diffusion length as a function of charge density for the same set of input parameters, however, their equivalence has not been tested before. **Fig.1** shows that for a cell with good performance, where the short circuit photocurrent is only decreased by 0.5% corresponding to a 99.5% steady-state collection efficiency, all three methods result in the same values for the diffusion length as a function of charge density. As was mentioned before, the measured diffusion length (Method 2) was calculated by simulation of a SLIT experiment to calculate the diffusion coefficient and by assuming a recombination rate from **Eq.3** at a given charge density. The measured diffusion coefficient was calculated using $D_m = d^2/3.54 \tau_m$ instead of the Nakade relation $D_m = d^2/2.77 \tau_m$.²⁵ As can be seen in the ESI, if the factor 3.54 is used instead of 2.77, the three methods give the same diffusion coefficient for the parameters in **Fig.1**.

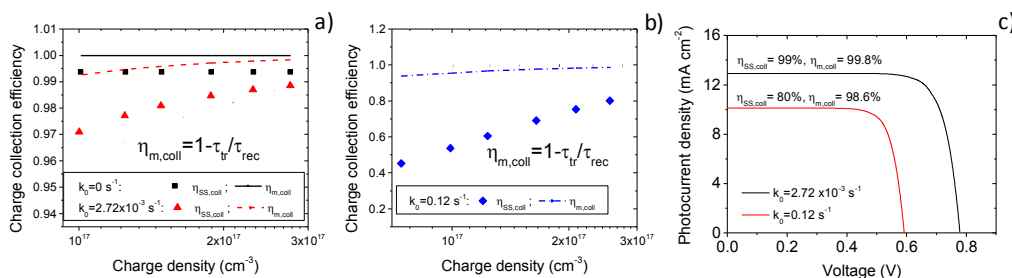


Fig. 4 Charge collection efficiency as a function of charge density for various recombination rates under short circuit conditions and current-voltage curves. The symbols represent the steady state collection efficiency while the lines correspond to the measured small perturbation collection efficiency: a) $k_0=0\text{ s}^{-1}$ (black squares) and $k_0=2.72\times 10^{-3}\text{ s}^{-1}$ (red triangles); b) $k_0=0.12\text{ s}^{-1}$ (blue diamonds). c) effect of recombination under short circuit conditions on the current-voltage curves.

It should be noted that this factor is a function of the absorption coefficient and the collection efficiency, and the original value was obtained from a simplified continuity equation with linear diffusion and recombination terms.²⁷ This correction of the pre-factor does not affect the slope of the diffusion coefficient and, hence, the validity of the comparison between methods that we carry out here.

From **Fig.1** it can be concluded that for the well-performing solar cell used here as a benchmark, the three methods to obtain the diffusion length are equivalent. However, that does not guarantee that extraction of these parameters is correct for all kinds of devices. Hence, the following questions need to be answered: how does recombination at short circuit affect the measured diffusion coefficient, the measured diffusion length, and the measured small perturbation collection efficiency in solar cells when the collection of carriers is not so efficient?

The first question can be addressed as follows: **Fig.2** shows the effect of recombination under short circuit conditions on the diffusion coefficient. When $k_0 = 2.72\times 10^{-3}\text{ s}^{-1}$ or smaller, the measured diffusion coefficient (Method 2) agrees with the value obtained from a calculation using the small perturbation equation (Method 1),¹⁵ $D=D_0(n/n_0)^{1/\alpha-\alpha}$. However, when the recombination rate constant is 44-fold larger the measured diffusion coefficient (Method 2) is overestimated, and this overestimation increases with decreasing charge density. This effect also leads to a different slope of the diffusion coefficient versus charge density graph, which could be interpreted as a different trap distribution parameter. Because the trap distribution parameter used is $\alpha = 0.286$ for all results in **Fig.2**, the different trap distribution parameter of $\alpha' = 0.333$ can be erroneously interpreted as an “activity factor” of 1.2. The activity factor has been reported in the literature as the value for the trap distribution parameter obtained from the D vs n plot divided by the value for α determined from a V_{oc} vs. n plot (See ESI for the experimental α found in this study). Possible origins of this activity factor have been described before. In one case, an activity factor higher than one was interpreted as a non-ideal thermodynamic behavior of electrons in the nanostructured two-phase system.^{28,29} Alternatively, it has been argued that the activity factor is related to a shift of the TiO_2 band edges with increasing electron concentration.³⁰ An important conclusion of this study is that the discrepancy between trap parameters obtained from independent

measurements of V_{oc} and D may be explained as being due to a contribution of recombination under short circuit conditions; to our knowledge, this explanation has not been considered before.

The second question refers to the diffusion length: **Fig.3** shows the influence of a 20% reduction in the short circuit current density due to recombination on the diffusion length determined by the three methods outlined above. It is observed that significant recombination under short circuit conditions leads to very different results for the three methods. Assuming that L_{Av} (Method 3) gives the *real* value for the diffusion length, we can draw the following conclusions: 1) The measured diffusion length L_m (Method 2) overestimates the real diffusion length L_{Av} ; 2) On the other hand, the small perturbation diffusion length L_{SP} (Method 1) underestimates the real value. Differences are also observed in the slope of the log-log plots of the diffusion length vs. charge density. From the small perturbation approximation (Method 1; **Eq.2**), we can observe that the slope is defined by the trap distribution ($\alpha = 0.286$) and the non-linear recombination ($\beta = 0.570$) parameters, leading to a slope of 0.752 which coincides with the value obtained for L_{SP} in **Fig.3**. **Fig.3** shows that for L_m the slope is 0.63 and for L_{Av} the slope is 0.197. Those differences in slope can be related with the effect of recombination under short circuit conditions. From **Fig.2** we can observe that the apparent trap distribution parameter (due to the apparent activity factor) is $\alpha' = 0.333$ and $\beta = 0.570$ (the same value for β is used for all calculations on this work). Using these values and **Eq.2**, we obtain a slope of 0.646, which is very similar to the value obtained for L_m in **Fig.3**. For the real diffusion length, L_{Av} , the slope is 0.197, which seems to have no explanation in terms of the trap distribution (0.286) and non-linear recombination parameters (0.570). Note that Method 3 is the only method that takes the effect of an electron density profile via **Eq.6** explicitly into account. This may result in a weaker dependence of the diffusion length on the total density (note that recombination takes place locally, at each x -position).

The third important parameter that we have analyzed is the collection efficiency. **Fig.4a** shows the effect of recombination under short circuit conditions on the charge collection efficiency. In the absence of recombination at short circuit ($k_0=0$), the steady state collection efficiency $\eta_{SS, coll}$ does not depend on charge density or light intensity, as expected. Contrary to this, when recombination slightly reduces the

$\eta_{SS, coll}$ by 0.5% at the highest light intensity (1 sun or $n \approx 2.8 \times 10^{17} \text{ cm}^{-3}$), i.e., a 0.5% decrease in the short circuit photocurrent, $\eta_{SS, coll}$ starts to depend on light intensity. At the lowest light intensity considered here (0.01 sun or $n \approx 1 \times 10^{17} \text{ cm}^{-3}$) $\eta_{SS, coll}$ has decreased by 2%, meaning that there is a 2% decrease in the short circuit photocurrent at this light intensity with respect to the situation where there is no recombination loss. As a consequence, measuring the short circuit photocurrent as a function of light intensity provides a method to determine whether recombination occurs under short circuit conditions; if recombination is significant this would be reflected by a slope that is not equal to 1. **Fig. 4b** shows the effect of recombination under short circuit conditions when the recombination rate constant is 44-fold higher, i.e., when k_0 is increased from $2.72 \times 10^{-3} \text{ s}^{-1}$ to 0.12 s^{-1} . At the highest light intensity (1 sun or $n \approx 2.8 \times 10^{17} \text{ cm}^{-3}$) the difference between the $\eta_{SS, coll}$ for $k_0 = 0 \text{ s}^{-1}$ (black squares) and $k_0 = 0.12 \text{ s}^{-1}$ (blue diamonds) is around 20%, whereas at the lowest light intensity (0.01 sun or $n \approx 1 \times 10^{17} \text{ cm}^{-3}$) the difference is around 50%. **Fig. 4** also compares the measured small perturbation collection efficiency, $\eta_{m, coll} = 1 - \tau_{tr}/\tau_{rec}$ (lines), with the steady state charge collection efficiency. As can be observed in **Fig. 4**, in all the cases $\eta_{m, coll}$ is close to 100% even when recombination significantly affects the short circuit photocurrent. This is a very common result when collection efficiencies are derived from small perturbation times, i.e. when the formula $1 - \tau_{tr}/\tau_{rec}$ is used. In all cases the collection efficiency is overestimated when small-perturbation techniques are used to calculate η_{coll} . The extent of the overestimation increases for a larger recombination rate under short circuit conditions (**Fig. 4b**). Finally, in **Fig. 4c** we compare the current-voltage curves for the two cases presented in **Fig. 4a** and **Fig. 4b**: 1) when the short-circuit photocurrent decreases by 0.5% due to recombination ($k_0 = 2.72 \times 10^{-3} \text{ s}^{-1}$); and 2) when the short-circuit photocurrent decreases by 20% due to recombination ($k_0 = 0.12 \text{ s}^{-1}$). In **Fig. 4c** similar parameters were used for both curves (Experimental parameters on **Fig. 1**) with the only difference being the recombination rate in dark, k_0 . The results unequivocally show that for the case where the steady-state collection efficiency is only 80%, that the small perturbation collection efficiency is still found to be close to 100%, illustrating that if recombination under short circuit conditions is significant, that small perturbation methods are not capable to accurately determine the steady-state collection efficiency. This shows that a particular device could be erroneously labeled as “very high collection efficiency” when the real recombination loss is far from negligible.

On the other hand, transport and recombination properties of solar cells are generally measured either under short circuit (IMPS, SLIT of photocurrent) or open circuit (IMVS, EIS, SLIT of photovoltage) conditions, but these are not the real working conditions of a solar cell. Nissfolk et al.³¹ studied transport/recombination of electrons in DSSCs under working conditions at the maximum power point. However, this situation is out of the scope of the present work, which is mainly focused on the influence of recombination processes occurring under short-circuit conditions. In future work, we

plan to expand the scope of this work to maximum power conditions.

To conclude, when recombination is negligible at short circuit, a good agreement between the results from the small perturbation approximation, the measured small perturbation values and the real diffusion length was found. In contrast, when recombination affects the performance even slightly, a dependence of the charge collection efficiency with illumination intensity is observed. This can be experimentally observed when the slope of a plot of the short circuit current density vs. light intensity is different from 1. A second method to analyze if recombination at short circuit is important is by comparing the value for α determined from the slope from the D vs. n plot with that determined from a V_{oc} vs. n plot: the larger the apparent activity factor, the more important the effect of recombination at short circuit. Finally, we point out that when the charge collection efficiency is 80% (at short circuit and under 1 sun illumination intensity) an overestimation of the diffusion coefficient, diffusion length, and collection efficiency as measured by small perturbation techniques is found. As a consequence, information obtained from small perturbation techniques should be taken with reserve when recombination at short circuit is present, especially for novel concept solar cells.

Acknowledgements

The authors gratefully acknowledge CONACYT for funding under Grant number CB-2012-178510, and for funding through the Mexican Center for Innovation in Solar Energy (CeMIE-Sol), Project P-27. We thank Junta de Andalucía for financial support via grant FQM 1851 and Ministerio de Economía y Competitividad of Spain under grant MAT2013-47192-C3-3-R. We also thank VIEP-BUAP for financial support.

Notes and references

- G. Schlichthörl, N. G. Park, and A. J. Frank. *J. Phys. Chem. B*, 1999, **103**, 782-791.
- J. Bisquert. *J. Phys. Chem. B*, 2002, **106**, 325-333
- L. Bertoluzzi and S. Ma. *Phys. Chem. Chem. Phys.*, 2013, **15**, 4283-4285.
- V. Sivaram, J. Kirkpatrick and H. J. Snaith. *J. Appl. Phys.*, 2013, **113**, 063709.
- E. Guillen, F. J. Ramos, J. A. Anta and S. Ahmad. *J. Phys. Chem. C* 2014, **118**, 22913-22922.
- A. Pockett, G. E. Eperon, T. Peltola, H. J. Snaith, A. Walker, L. M. Peter and P. J. Cameron. *J. Phys. Chem. C*, 2015, **119**, 3456-3465.
- Y. Zhao, and K. Zhu. *J. Phys. Chem. Lett.*, 2013, **4**, 2880-2884.
- Y. Zhao, A. M. Nardes, and K. Zhu. *J. Phys. Chem. Lett.* 2014, **5**, 490-494.
- M. M. Lee, J. Teuscher, T. Miyasaka, T. N. Murakami and H. J. Snaith. *Science* 2012, **338**, 643-647.
- D. Bi, L. Yang, G. Boschloo, A. Hagfeldt and E. M. J. Johansson. *J. Phys. Chem. Lett.*, 2013, **4**, 1532-1536.
- H. S. Kim, et. al. *Nature comm.*, 2013, **4**, 2242.
- A. Dualeh, T. Moehl, N. Tétreault, J. Teuscher, P. Gao, M. K. Nazeeruddin and M. Grätzel. *ACS Nano*, 2014, **8**, 362-373.

- 13 B. C. O'Regan, P. R. F. Barnes, X. Li, C. Law, E. Palomares and J. M. Marin-Beloqui. *J. Am. Chem. Soc.*, 2015, **137**, 5087-5099.
- 14 A. Todinova, J. Idígoras, M. Salado, S. Kazim and J. A. Anta. *J. Phys. Chem. Lett.*, 2015, **6**, 3923-3930.
- 15 J. A. Anta, J. Idígoras, E. Guillén, J. Villanueva-Cab, H. J. Mandujano-Ramírez, G. Oskam, L. Pellejàc and E. Palomares. *Phys. Chem. Chem. Phys.*, 2012, **14**, 10285-10299.
- 16 L. M. Peter. *J. Phys. Chem. C*, 2007, **111**, 6601-6612.
- 17 J. Nissfolk, K. Fredin, J. Simiyu, L. Häggman, A. Hagfeldt and G. Boschloo. *J. Electroanal. Chem.*, 2010, **646**, 91-99.
- 18 J. A. Anta, F. Casanueva, and G. Oskam. *J. Phys. Chem. B*, 2006, **110**, 5372-5378.
- 19 J. Villanueva-Cab, G. Oskam, J. A. Anta. *Solar Energy Materials & Solar Cells*, 2010, **94**, 45-50.
- 20 J. Villanueva, J. A. Anta, E. Guillen and G. Oskam. *J. Phys. Chem. C*, 2009, **113**, 19722-19731.
- 21 J. Villanueva-Cab, H. Wang, G. Oskam, and L. M. Peter. *J. Phys. Chem. Lett.*, 2010, **1**, 748-751.
- 22 S. D. Stranks, G. E. Eperon, G. Grancini, C. Menelaou, M. J. P. Alcocer, T. Leijtens, L. M. Herz, A. Petrozza, and H. J. Snaith. *Science*, 2013, **342**, 341-344.
- 23 E. Amaldi and E. Fermi. *Phys. Rev.*, 1936, **50**, 899-927.
- 24 J. Bisquert and I. Mora-Seró. *J. Phys. Chem. Lett.*, 2010, **1**, 450-456.
- 25 S. Nakade, T. Kanzaki, Y. Wada and S. Yanagida. *Langmuir*, 2005, **21**, 10803-10807.
- 26 G. Schlichthörl, N. G. Park and A. J. Frank. *J. Phys. Chem. B*, 1999, **103**, 782-791.
- 27 L. Dloczik, O. Ilerperuma, I. Lauer mann, L. M. Peter, E. A. Ponomarev, G. Redmond, N. J. Shaw, and I. Uhlendorf. *J. Phys. Chem. B*, 1997, **101**, 10281-10289.
- 28 J. R. Jennings, A. Ghicov, L. M. Peter, P. Schmuki and A. B. Walker. *J. Am. Chem. Soc.*, 2008, **130**, 13364-13372.
- 29 E. Guillén, L. M. Peter and J. A. Anta. *J. Phys. Chem. C*, 2011, **115**, 22622-22632.
- 30 P. R. F. Barnes, A. Y. Anderson, J. R. Durrant, and B. C. O'Regan. *Phys. Chem. Chem. Phys.*, 2011, **13**, 5798-5816.
- 31 J. Nissfolk, K. Fredin, A. Hagfeldt and G. Boschloo. *J. Phys. Chem. B*, 2006, **110**, 36.